Optimal Sensor and Actuator Placement in Line Networks

Damiano La Manna, Adriano Fagiolini, Fabio Pasqualetti

Abstract— **This letter investigates the problem of optimal sensor location in network systems. We study the problem of detecting unknown disturbances in network systems, and we particularly focus on the case of line networks. We adopt a measure based on the network *cross-Gramian* to evaluate different sensor locations with respect to the origin of the signal to be detected. We consider both the cases of Toeplitz line networks, where the edge weights are specified by three parameters, and line networks with general weights. As a counterintuitive result we prove that, depending on the edge weights, the sensor should be placed as far as possible in the network from the origin of the signal. On the other hand, in certain regions of the parameter space, the sensor should be co-located with the signal to be detected. Our results suggest that sensor location methods based on the network topology alone may lead to poor detection performance in complex cyber-physical systems, due to the intricate relation between the system dynamics and the underlying network structure. The findings are illustrated on a class of electronic circuits.**

I. Introduction

Network systems are prone to malicious attacks and faults against individual nodes and interconnection dynamics. Perturbations propagate across components and subnetworks, and may cascade into the failure of all interconnected parts [1]. Reliable operation of network systems relies on the prompt detection and remedy of malfunctions.

The ability to detect perturbation in network systems depends on the the intrinsic structure of the system, as well as on the location of sensors and monitors. In this letter we focus on the latter aspect, and we try to identify optimal network locations for the detection of an unknown perturbation signal. In particular, we define detection metrics based on the *static gain* of the dynamical network system [2]. We consider a class of network systems with line interconnection structure, and we identify optimal sensor locations based on the network weights and the origin of the perturbation signal. Surprisingly we find that, in some cases, sensors should be located as far as possible from the origin of the perturbation while, in other cases, the distance between the sensors and the origin of the perturbation should be minimized. Although our results pertain a specific, and simple, interconnection structure, we conjecture that a similar behavior may appear in more complex interconnection structures, and that novel techniques are necessary to relate the structure with the dynamical properties of the associated network system.

This material is based upon work supported by awards UCOP-LFR-18-548175, AFOSR-FA9550-19-1-0235, and ARO-71603NSYIP. D. La Manna and A. Fagiolini are with the Department of Engineering, University of Palermo, Italy, {damiano.lamanna, fagiolini}@unipa.it. F. Pasqualetti is with the Mechanical Engineering Department, University of California at Riverside, fabiopas@engr.ucr.edu.

Related work The problem of selecting sensors and actuators in dynamical systems has received considerable attention in the controls community. Typically, sensors and actuators are selected to maximize, respectively, certain observability and controllability metrics, often quantified by Gramian matrices [3], [4], [5]. For small-scale problems, the maximization of observability and controllability metrics often relies on combinatorial procedures, which do not offer any particular insight into the structure of the problem, and become computationally infeasible for large problems.

Motivated by a renewed interest in network systems, and particularly by the need for a deepened understanding of the relation between network structure and network dynamics, recent studies have focused on determining suitable optimization metrics for sensor and actuator placement in large-scale systems [6], as well as on highlighting tradeoffs and relations between network structure and the associated Gramians [7], [8], [9]. In a related fashion, the controllability Gramian has been analyzed for security and synchronization problems in network systems [10], [11]. In this letter, we continue the work along these directions by considering the trace of the cross-Gramian [2] as a metric for joint sensor and actuator location in network systems, and by providing explicit results for a class of network systems under the hypothesis that the input attack location is a priori known (see e.g. [12]).

Contributions We define a sensor location problem for network systems, and we use the trace of the cross-Gramian or, equivalently for single-input single-output systems, the system static gain, to evaluate different sensor locations with respect to the location of a perturbation signal. We consider network systems with tridiagonal adjacency matrix (line networks), and we separately analyze the cases of Toeplitz and general edge weights. For the case of Toeplitz line networks, we uniquely identify optimal sensor locations with respect to the edge weights. This result is obtained by characterizing the behavior of the entries of the inverse of the network adjacency matrix, which may increase or decrease as a function of the network cardinality. Additionally we prove that a similar result is achieved in certain regions of the parameter space also for the case of line networks with general weights. A numerical study validates our findings.

II. Problem statement and preliminary results

In this section we detail our setup and introduce preliminary concepts that will be used throughout the rest of the letter. Consider a network represented by an interconnection graph $\mathcal{G} = (\mathcal{V}, \mathcal{E})$, where $\mathcal{V} = \{1, \cdots, n\}$ and $\mathcal{E} \subseteq \mathcal{V} \times \mathcal{V}$ denote the vertex and edge sets, respectively, and a weighted adjacency matrix $A \in \mathbb{R}^{n \times n}$ containing the weights of the

network interconnection edges. That is, $A = [a_{ij}]$, where $a_{ij} = 0$ if $(i,j) \notin \mathcal{E}$, and a_{ij} equals the weight of the edge (i,j) otherwise. Assume that a subset of vertices $\mathcal{U} \subseteq \mathcal{V}$, with $|\mathcal{U}| = m$, is affected by an external and unknown signal representing genuine disturbances or malicious attacks, and that a subset of nodes $\mathcal{Y} \subseteq \mathcal{V}$, with $|\mathcal{Y}| = p$, is equipped with sensors capable of measuring the nodes activity. Let $B \in \mathbb{R}^{n\times m}$ be the submatrix of the n-dimensional identity matrix with columns indexed by $\mathcal{U}$, and let $C \in \mathbb{R}^{p\times n}$ be the submatrix of the n-dimensional identity matrix with rows indexed by $\mathcal{Y}$. Let $x_i \in \mathbb{R}$ be the state associated with node i.

We assume that the network systems evolves according to linear, continuous-time dynamics described by its weighted adjacency matrix, that is,

$$\dot{x}(t) = A\,x(t) + B\,u(t), \quad y(t) = C\,x(t), \tag{1}$$

where $x = (x_1, \cdots, x_n)^T$, $u = (u_1, \cdots, u_m)^T$, and $y = (y_1, \cdots, y_p)^T$ are the network state vector, the unknown disturbance input, and the measured output vector, respectively.

Two dual problems are of interest. On the one hand, based on the knowledge of the network dynamics A and sensor locations $\mathcal{Y}$, an *attacker* aims to find optimal input vertices $\mathcal{U}$ to maximally disrupt the network system while preventing observability from the sensor nodes. Conversely, based on the knowledge of the network dynamics A and input locations $\mathcal{U}$, the objective of a security system is to determine the sensor nodes $\mathcal{Y}$ ensuring optimal detectability of an unknown disturbance. The two problems can be addressed independently by defining quantitative notions of controllability and observability for the network system [3]. Yet, an approach combining both structural measures may lead to more robust results [13]. To this aim, we adopt the notion of *cross-Gramian* that was first introduced for single-input single-output linear systems in [14], and then extended for the multi-input multi-output case in [15]:

Definition 2.1: ***(cross-Gramian)*** For a stable network system described by the triple (A, B, C), the cross-Gramian is defined as

$$W_{co} = \int_0^\infty e^{At}\,B\,C\,e^{At}\,dt\,,$$

or, equivalently, as the solution to the Sylvester's equation

$$A\,W_{co} + W_{co}\,A = -B\,C\,.$$

As shown in [14], the cross-Gramian matrix W_{co} carries information about both controllability and observability of the network. For symmetric systems, the cross-Gramian is indeed related to the controllability and observability Gramians, W_c and W_o, by the relation $W_{co} = \sqrt{W_c\,W_o}$ [2], [16]. Moreover, for single-input single-output systems, the trace of the cross-Gramian is related to the network steady-state gain $g = -\,C\,A^{-1}\,B$ by the equation[15]

$$\text{Trace}\,(W_{co}) = \tfrac{1}{2}\,g\,. \tag{2}$$

Eq. 2 suggests that Trace(W_{co}) can in fact be used to evaluate the amplification or attenuation of a network signal that is slowly varying with respect to the network dynamics. Motivated by the above discussion, in this letter we focus on the following problem:

Problem 2.1: ***(Optimal sensor placement)*** Given a network $\mathcal{G}$ with adjacency matrix A, input nodes $\mathcal{U}$, and dynamics as in (1), determine the sensor locations $\mathcal{Y}$, with $|\mathcal{Y}| = p$, that maximize the trace of the associated cross-Gramian, i.e. $\max_{\mathcal{Y}} \text{Trace}(W_{co})$, subject to $|\mathcal{Y}| = p$. □

Addressing the above problem for generic networks, with possibly multiple input nodes and with several sensors, is a daunting task. In this letter we focus on a *single-attack, single-sensor* scenario, where $|\mathcal{U}| = 1$ and $|\mathcal{Y}| = 1$. Under this hypothesis, it can be shown that the trace of the cross-Gramian becomes

$$\text{Trace}\,(W_{co}) = -\tfrac{1}{2}A^{-1}_{ij}\,,$$

where A^{-1}_{ij} is (i,j)-th entry of the inverse of the adjacency matrix A. Thus, for the single-input single-sensor case, Prob. 2.1 can be addressed by characterizing the inverse of the network adjacency matrix, so as to select the node i that maximizes the element A^{-1}_{ij}. This solution strategy is used in the next section to determine optimal sensor location in line networks, and to show that the network structure and dynamics may enforce counterintuitive relations regarding the location of sensors and actuators in a complex system.

III. Optimal Sensor Placement for Line Networks

A. Toeplitz Line Networks

Consider a Toeplitz line network with a tridiagonal adjacency matrix where the coefficients $a, b, c \in \mathbb{R}_{\neq 0}$:

$$A = \begin{pmatrix} a & b & \cdots & 0 & 0 \\ c & a & \cdots & 0 & 0 \\ \vdots & \vdots & \ddots & \vdots & \vdots \\ 0 & 0 & \cdots & a & b \\ 0 & 0 & \cdots & c & a \end{pmatrix}. \tag{3}$$

It is known that the inverse $A^{-1} = [A^{-1}_{ij}]$ of a tridiagonal Toeplitz matrix A is given by [17]:

$$A^{-1}_{ij} = \frac{1}{\theta_n}\begin{cases} (-1)^{i+j} b^{j-i}\,\theta_{i-1}\,\phi_{j+1}, & \text{for } i \le j\,, \\ (-1)^{i+j} c^{i-j}\,\phi_{i+1}\,\theta_{j-1}, & \text{for } i > j\,, \end{cases} \tag{4}$$

where the coefficients θ_k are obtained through the forward iteration

$$\theta_k = a\,\theta_{k-1} - bc\,\theta_{k-2} \text{ for } k = 2, \cdots, n\,, \tag{5}$$

with initial conditions $\theta_0 = 1$ and $\theta_1 = a$, while the coefficients ϕ_k are computed through the backward iteration

$$\phi_k = a\,\phi_{k+1} - bc\,\phi_{k+2} \text{ for } k = n-1, \cdots, 1\,, \tag{6}$$

with final conditions $\phi_{n+1} = 1$ and $\phi_n = a$. It can be shown that $\theta_n = \det(A)$.

In this framework we are interested in characterizing the behavior of the sequences (5) and (6) for large networks. For this reason, even though the network cardinality is finite, we adopt the following asymptotic definitions:

Definition 3.1: ***(Decreasing sequence)*** A sequence $m(j)$, with $j = 1, 2, \ldots$, is *decreasing* if there exist j^*, $\gamma \in \mathbb{R}_{>0}$ and $\rho \in (0,1)$ satisfying $|m(j)| \le \gamma\rho^j$ for $j \ge j^*$. □

Definition 3.2: ***(Increasing sequence)*** A sequence $m(j)$, with $j = 1, 2, \ldots$, is *increasing* if there exist j^*, $\gamma \in \mathbb{R}_{>0}$ and $\rho \in \mathbb{R}_{>1}$ satisfying $|m(j)| \geq \gamma \rho^j$ for $j \geq j^*$. □

The following theorem characterizes the behavior of the entries A^{-1}_{ij} of the inverse of a tridiagonal Toeplitz matrix A.

Theorem 3.1: ***(Inverse of Toeplitz matrix)*** Let $A \in \mathbb{R}^{n\times n}$ be a tridiagonal Toeplitz matrix with parameters $a, b, c \in \mathbb{R}_{\neq 0}$. Let

$$\mu_+ = -a + \sqrt{a^2 - 4bc}, \text{ and } \mu_- = -a - \sqrt{a^2 - 4bc}.$$

As the dimension n grows, the entries A^{-1}_{ij} satisfy the following conditions:

1) For all rows i,
   a) if $|\mu_+| < 2|b|$ and $|\mu_-| < 2|b|$, then the sequence A^{-1}_{ij}, with $j \geq i$, is increasing;
   b) if $|\mu_+| > 2|b|$ or $|\mu_-| > 2|b|$, then the sequence A^{-1}_{ij}, with $j \geq i$, is decreasing;
2) For all rows i,
   a) if $|\mu_+| < 2|c|$ and $|\mu_-| < 2|c|$, then the sequence A^{-1}_{ij}, with $j < i$, is decreasing;
   b) if $|\mu_+| > 2|c|$ or $|\mu_-| > 2|c|$, then the sequence A^{-1}_{ij}, with $j < i$, is increasing.

Proof: To analyze the behavior of the entries of A^{-1}, based on (4), one can conveniently fix a row index i and study the behavior of all column entries j by distinguishing the cases with $i \leq j$ and $i > j$.

If $i \leq j$, the entry A^{-1}_{ij} can be factorized as

$$y^i(j) := A^{-1}_{ij} = \alpha(i)\,(-1)^j\, b^j \phi(j+1)\,,$$

where $\alpha(i) = (-1)^i\, b^{-i}\, \theta_n^{-1}\, \theta_{i-1}$. Starting from the last two column entries, which are given by

$$\begin{aligned} y^i(n) &= \alpha(i)\,(-1)^n\, b^n\,, \\ y^i(n-1) &= \alpha(i)\,(-1)^{n-1}\, b^{n-1} a\,, \end{aligned}$$

one can recursively obtain all other entries of the i-th row through a backward recurrence relation that is derived below. Consider expanding the expression of the entry $y^i(j-1)$ as follows: for $j = n, \cdots, i+1$,

$$\begin{aligned} y^i(j-1) &= \alpha(i)\,(-1)^{j-1}\, b^{j-1}\, \phi(j) \\ &= \alpha(i)\,(-1)^{j-1}\, b^{j-1}\, (a\,\phi(j+1) - bc\,\phi(j+2)) \\ &= -\tfrac{a}{b}\, y^i(j) - \tfrac{c}{b}\, y^i(j+1)\,. \end{aligned}$$

Translating of a step backward the above relation yields: $y^i(j-2) = -\frac{c}{b}\, y^i(j) - \frac{a}{b}\, y^i(j-1)$, for $j = n+1, \cdots, i+2$. To analyze the behavior of the above difference equation, one can define the vector state $x(j) = \big(y^i(j), y^i(j-1)\big)^T$, whose backward evolution is described by the state form

$$x(j-1) = H_\phi\, x(j)\,, \text{ for } j = n, \cdots, i+2\,, \qquad (7)$$

with $H_\phi = \begin{pmatrix} 0 & 1 \\ -c/b & -a/b \end{pmatrix}$, and initial condition $x(n) = \alpha(i)\,(-1)^n(-b^{n+1}, b^n a)^T$. Based on the expression of H_ϕ's eigenvalues, that are $\mu_+/2b$ and $\mu_-/2b$, one can conclude the following. 1-a) If $|\mu_+| < 2\,|b|$ and $|\mu_-| < 2\,|b|$, both eigenvalues lay inside the unit circle, the backward evolution of the system in (7) is decreasing, while the sequence $\{y^i(j)\}$, for $j = i, i+1, \cdots, n$, is increasing. 1-b) If $|\mu_+| > 2\,|b|$ and $|\mu_-| > 2\,|b|$, at least one eigenvalue lays outside the unit circle, the backward evolution of the system in (7) is increasing, and the sequence $\{y^i(j)\}$ is decreasing.

If $i > j$, the entry of A^{-1}_{ij} can be factorized as

$$y^i(j) := A^{-1}_{ij} = \beta(i)\,(-1)^j\, c^{-j}\, \theta(j-1)\,,$$

where $\beta(i) = (-1)^i\, c^i\, \theta_n^{-1}\, \phi_{i+1}$. Starting from the first two column entries, $y^i(1) = -\beta(i)/c$ and $y^i(2) = \beta(i)\,a/c^2$, one can recursively obtain all other entries of the i-th row through a forward recurrence relation that is derived below. Consider expanding the expression of the entry $y^i(j+1)$ as follows: for $j = 2, \cdots, n$,

$$\begin{aligned} y^i(j+1) &= \beta(i)\,(-1)^{j+1}\, c^{-j-1}\, \theta(j) \\ &= \beta(i)\,(-1)^{j+1}\, c^{-j-1}\, (a\,\theta(j-1) - bc\,\theta(j-2)) \\ &= -\tfrac{a}{c}\, y^i(j) - \tfrac{b}{c}\, y^i(j-1)\,. \end{aligned}$$

Translating of a step forward the above relation yields $y^i(j+2) = -\frac{b}{c}\, y^i(j) - \frac{a}{c}\, y^i(j+1)$ for $j = 1, \cdots, n-1$. One can define the vector state $x(j) = \big(y^i(j), y^i(j+1)\big)^T$ and study the evolution of the state form

$$x(j+1) = H_\theta\, x(j)\,, \text{ for } j = 1, \cdots, i-1\,, \qquad (8)$$

with $H_\theta = \begin{pmatrix} 0 & 1 \\ -b/c & -a/c \end{pmatrix}$, and initial condition $x(1) = \beta(i)\,(1, a)^T$. Based on the expression of H_θ's eigenvalues, that are $\mu_+/2c$ and $\mu_-/2c$, one can conclude the following. 2-a) If $|\mu_+| < 2\,|c|$ and $|\mu_-| < 2\,|c|$, both eigenvalues lay inside the unit circle and the sequence $\{y^i(j)\}$, for $j = i, i+1, \cdots, n$, is decreasing. 2-b) If $|\mu_+| > 2\,|c|$ and $|\mu_-| > 2\,|c|$, at least one eigenvalue lays outside the unit circle and the sequence $\{y^i(j)\}$ is increasing. ■

Th. 3.1 characterizes the behavior of the sequences defined by the entries of the rows of A^{-1}. Fig. 1 contains graphical illustrations of the possible trends that may occur depending on the network parameters a, b, c. The theorem can be used to describe an optimal sensor location, and indeed to solve for Prob. 2.1, for tridiagonal Toeplitz networks. The following corollary can be established under the hypothesis that the designer has a priori knowledge of the location of the input node (e.g., see [12]).

Corollary 3.1: ***(Optimal sensor placement for Toeplitz networks)*** Consider a Toeplitz line network as in (1). If the input is located at node j, then the sensor node i such that A^{-1}_{ij} is largest is determined as follows:

1) If 1-a and 2-a hold, then $i = j$, that is, the sensor is co-located with the input node;
2) if 1-b and 2-a hold, then $i = 1$, that is, the sensor is located at the first node;
3) if 1-a and 2-b hold, then $i = n$, that is, the sensor is located at the last node of the line;
4) if 1-b and 2-b hold, then $i = h$, where h is the nearest between 1 and n to vertex j, i.e.,

$$h = \begin{cases} 1 \text{ if } j \leq \frac{n}{2}\,, \\ n \text{ if } j > \frac{n}{2}\,, \end{cases} \quad h = \begin{cases} 1 & \text{if } j \leq \left\lfloor \frac{n}{2} \right\rfloor\,, \\ n & \text{if } j > \left\lceil \frac{n}{2} \right\rceil\,, \\ 1 \text{ or } n & \text{if } j = \left\lceil \frac{n}{2} \right\rceil\,. \end{cases}$$

(if n is even) (if n is odd)

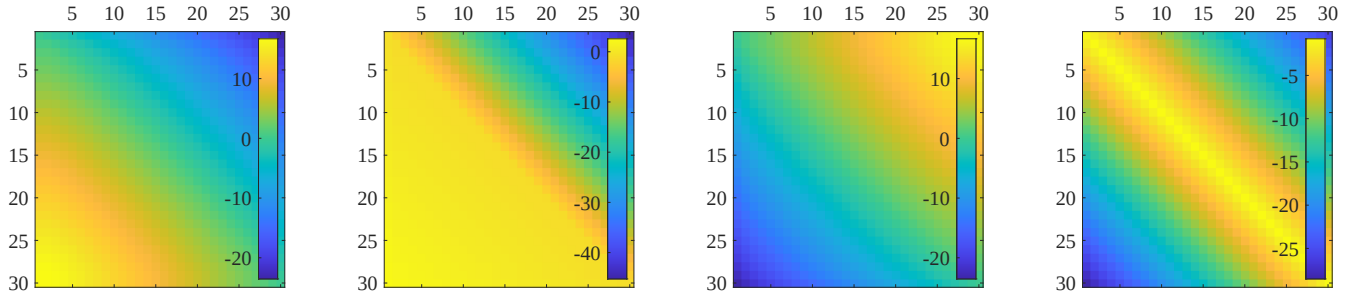

$(a)\ a=-2, b=0.5, c=2$ $(b)\ a=-2, b=0.6, c=-3$ $(c)\ a=-2, b=2, c=0.5$ $(d)\ a=-3, b=1.1, c=1$

Fig. 1. Heat maps of the matrix $\log(|A^{-1}|)$ for different tridiagonal Toeplitz matrix $A \in \mathbb{R}^{30\times 30}$ (brighter colors indicate entries with larger absolute values). Referring to Th. 3.1, (a) and (b) satisfy conditions 1-b and 2-a so that, for each row, the sequence of entries is decreasing, (c) satisfy conditions 1-a and 2-b so that, for each row, the sequence of entries is increasing, and (d) satisfy conditions 1-b and 2-b so that the sequence of entries is decreasing for $j \geq i$ and increasing for $j < i$. Notice that all matrices A are Hurwitz.

Proof: The proof trivially follows from Th. 3.1. ■

Remark 3.1: ***(Stability of the network matrix)*** It should be observed that the stability of a tridiagonal Toeplitz matrix A does not imply the convergence or divergence of the entries of its inverse A^{-1}. In fact, Th. 3.1 shows that, even for stable matrices, the rows of the inverse of the network matrix may contain convergent or divergent sequences of entries. See Sec. IV for an example. □

B. General Line Networks

Let us now focus on the case of general line networks described by tridiagonal adjacency matrices of the form:

$$A = \begin{pmatrix} a_1 & b_1 & \cdots & 0 & 0 \\ c_1 & a_2 & \cdots & 0 & 0 \\ \vdots & \vdots & \ddots & \vdots & \vdots \\ 0 & 0 & \cdots & a_{n-1} & b_{n-1} \\ 0 & 0 & \cdots & c_{n-1} & a_n \end{pmatrix}, \tag{9}$$

with coefficients $a_k, b_k, c_k \in \mathbb{R}_{\neq 0}$ for all k. The formula for the entries of the inverse $A^{-1} = [A^{-1}_{i,j}]$ is generalized as follows [17]:

$$A^{-1}_{ij} = \frac{1}{\theta_n} \begin{cases} (-1)^{i+j}\, b_i \cdots b_{j-1}\, \theta_{i-1}\, \phi_{j+1}, & \text{for } i \leq j\,, \\ (-1)^{i+j}\, c_j \cdots c_{i-1}\, \phi_{i+1}\, \theta_{j-1}, & \text{for } i > j\,, \end{cases}$$

where the coefficients θ_k and ϕ_k are obtained respectively through the forward and backward iterations:

$$\begin{aligned} \theta_k &= a_k\, \theta_{k-1} - b_{k-1} c_{k-1}\, \theta_{k-2}\,, \text{ for } k = 2, \cdots, n\,, \\ \phi_k &= a_k\, \phi_{k+1} - b_k c_k\, \phi_{k+2}\,, \text{ for } k = n-1, \cdots, 1\,, \end{aligned}$$

with initial conditions respectively given by $\theta_0 = 1, \theta_1 = a_n$, and $\phi_{n+1} = 1, \phi_n = a_n$.

A complete characterization of the behavior of the inverse A^{-1} of a general tridiagonal matrix A is not immediate, and in fact involves conditions that cannot be easily verified. However, a conservative yet useful analysis test can be derived, based on lower and upper approximations of A by suitable tridiagonal Toeplitz matrices. This fact is shown in the following theorem.

Theorem 3.2: ***(Inverse of tridiagonal matrix)*** Let $A \in \mathbb{R}^{n\times n}$ be a tridiagonal matrix with parameters $a_i, b_i, c_i \in \mathbb{R}_{\neq 0}$. Let $\underline{a}, \underline{b}, \underline{c}, \bar{a}, \bar{b}, \bar{c} \in \mathbb{R}_{>0}$. Assume that

$$\begin{aligned} (\bar{a}^2 - 4\,\underline{b}\,\underline{c})\,(\bar{a}^2 - 4\,\underline{b}\,\bar{c}) > 0\,, \\ (\underline{a}^2 - 4\,\bar{b}\,\bar{c})\,(\underline{a}^2 - 4\,\bar{b}\,\underline{c}) > 0\,, \end{aligned} \tag{10}$$

and, for all indices i,

$$\underline{a} \leq |a_i| \leq \bar{a},\ \underline{b} \leq |b_i| \leq \bar{b},\ \underline{c} \leq |c_i| \leq \bar{c}.$$

Let $\nu_1 = \bar{a} + \sqrt{\bar{a}^2 - 4\,\underline{b}\,\underline{c}}$, and $\nu_2 = \underline{a} - \sqrt{\underline{a}^2 - 4\,\bar{b}\,\bar{c}}$.

As the dimension n grows, the entries A^{-1}_{ij} satisfy the following conditions:

1) For all rows i,
   a) if $|\nu_2| > 2\,\bar{b}$, then the sequence A^{-1}_{ij}, with $j \geq i$, is decreasing;
   b) if $|\nu_1| < 2\,\underline{b}$, then the sequence A^{-1}_{ij}, with $j \geq i$, is increasing.
2) For all rows i,
   a) if $|\nu_1| < 2\,\underline{c}$, then the sequence A^{-1}_{ij}, with $j < i$, is decreasing;
   b) if $|\nu_2| > 2\,\bar{c}$, then the sequence A^{-1}_{ij}, with $j < i$, is increasing.

Proof: As in Th. 3.1 one can conveniently fix a row index i and study the behavior of all column entries j for $i \leq j$ and $i > j$.

If $i \leq j$, the entry A^{-1}_{ij} can be factorized as

$$y^i(j) := A^{-1}_{ij} = \alpha'(i)\,(-1)^j\, b_i \cdots b_{j-1}\, \phi(j+1),$$

where $\alpha'(i) = (-1)^i\, \theta_n^{-1}\, \theta_{i-1}$. The entry $A^{-1}_{i,j-1}$ can be rewritten as follows:

$$\begin{aligned} y^i(j-1) &= -\alpha'(i)\,(-1)^j\, b_i \cdots b_{j-2}\, \phi(j) = \\ &= -\tfrac{a_j}{b_{j-1}}\, y^i(j) - \tfrac{c_j}{b_{j-1}}\, y^i(j+1)\,, \end{aligned}$$

and thus, after translating of a step backward, the following difference equation is obtained:

$$y^i(j-2) = -\tfrac{c_j}{b_{j-1}}\, y^i(j) - \tfrac{a_j}{b_{j-1}}\, y^i(j-1)\,,$$

for $j = n+1, \cdots, i+2$. One obtains the following column-dependent, backward state form that generalizes (7):

$$\begin{pmatrix} y^i(j-1) \\ y^i(j-2) \end{pmatrix} = \begin{pmatrix} 0 & 1 \\ -\frac{c_j}{b_{j-1}} & -\frac{a_j}{b_{j-1}} \end{pmatrix} \begin{pmatrix} y^i(j) \\ y^i(j-1) \end{pmatrix}, \tag{11}$$

for $j = n-1, \cdots, 2$, and whose dynamic matrix has the following column-dependent eigenvalues

$$\lambda_{1,2}^{(j)} = \frac{1}{2\,b_{j-1}} \left(-a_j \pm \sqrt{a_j^2 - 4\,b_{j-1}\,c_j} \right) .$$

If $i > j$, the entry A_{ij}^{-1} can be factorized as

$$y^i(j) := A_{ij}^{-1} = \beta'(i)\,(-1)^j\,c_j \cdots c_{i-1}\,\theta(j-1)\,,$$

where $\beta'(i) = (-1)^i\,\theta_n^{-1}\,\phi_{i+1}$, and one obtains the following column-dependent state form that generalizes (8):

$$\begin{pmatrix} y^i(j+1) \\ y^i(j+2) \end{pmatrix} = \begin{pmatrix} 0 & 1 \\ -\frac{b_{j-1}}{c_j} & -\frac{a_j}{c_j} \end{pmatrix} \begin{pmatrix} y^i(j) \\ y^i(j+1) \end{pmatrix} , \qquad (12)$$

for $j = 1, \cdots, i-1$, and whose dynamic matrix has the following column-dependent eigenvalues

$$\mu_{1,2}^{(j)} = \frac{1}{2\,c_j} \left(-a_j \pm \sqrt{a_j^2 - 4\,b_{j-1}\,c_j} \right) .$$

Under the conditions in (10), it is possible to find the following upper and lower bounds for the modules of the eigenvalues $\lambda_{1,2}^{(j)}$ and $\mu_{1,2}^{(j)}$: $\frac{|\nu_2|}{2\,\bar{b}} \leq |\lambda_{1,2}^{(j)}| \leq \frac{|\nu_1|}{2\,\underline{b}}$, $\frac{|\nu_2|}{2\,\bar{c}} \leq |\mu_{1,2}^{(j)}| \leq \frac{|\nu_1|}{2\,\underline{c}}$. As in Th. 3.1, when both eigenvalues $\lambda_{1,2}^{(j)}$ lay inside the unit circle, for all j, the backward dynamics in (11) is decreasing and the forward sequence $\{y^i(j)\}$ is increasing, while, when both eigenvalues $\mu_{1,2}^{(j)}$ lay inside the unit circle, for all j, the dynamics in (12) is decreasing and the same holds for the sequence $\{y^i(j)\}$. This reasoning explains the conditions in the statement of the theorem. ■

As for the case of Toeplitz line networks discussed in Th. 3.1, Th. 3.2 provides guidelines for the selection of sensor nodes with respect to the input location and the network parameters.

IV. Numerical Examples

In this section we validate our findings with two numerical examples. In particular, in Sec. IV-A we fix the diagonal entries of the network matrix, and plot the regions of the parameter space yielding decreasing and increasing behaviors of the entries of the network inverse matrix. In Sec. IV-B we present an electronic network whose dynamics is described by a tridiagonal matrix, and we analyze its steady-state behavior as a function of the network elements and the locations of the input and sensor nodes.

A. Map of decreasing and increasing parameters

Consider a line network as in Fig. 2, where an input affects the i-th node whose effect is measured from the j-th node. Let the network cardinality be $n = 30$ and the network's diagonal elements be $a = -0.3$. In Fig. 3 we report the parameter space regions corresponding to decreasing and increasing entries of the network's inverse matrix (see Th. 3.1). We now fix the network weights and assume that $i = 1$ and the signal injected into the network is a white noise with zero mean and unit variance. Fig. 3 again shows how the input signal is amplified at different nodes of the network, depending on the network weights. Results are consistent with the predictions from Th. 3.1.

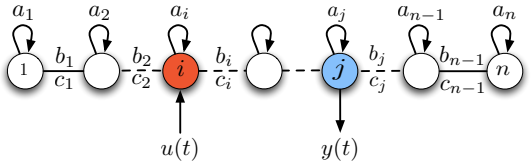

Fig. 2. Line network with n nodes. The i-th node is affected by an attack, and the j-th node represents the optimal sensor placement.

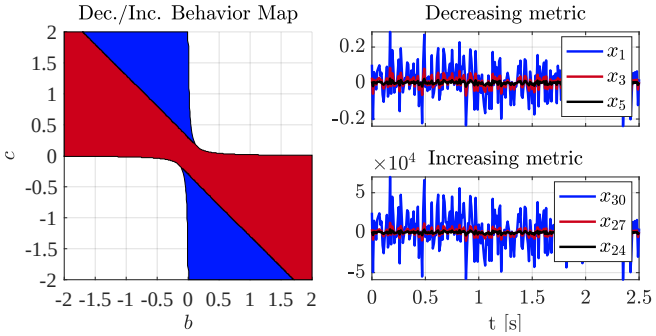

Fig. 3. Line network features: (left) convergence/divergence map for $a = -0.3$ and $-2 \leq b, c \leq 2$ (blue and red indicate regions where the sequence A_{ij}^{-1} is decreasing and increasing, respectively; white regions indicate unstable networks; the axes $b = 0$ and $c = 0$ are excluded since A not invertible); (right) simulation runs with two networks having a decreasing and increasing metric, respectively; the former is with $b = 0.57$ and $c = -1.37$ and has the input maximum amplification at node where it is applied, while the latter is with $b = 0.1$ and $c = 0.25$ maximally amplifies at the furthest node.

B. An electronic network yielding tridiagonal dynamics

Consider the electronic circuit in Fig. 4, which represents a multistage amplifier [18], and consists of a chain of RC elements connected by voltage-feedback transconductance amplifiers. The i-th part of the system, for $i = 1, \cdots, n$, includes a resistor R_i, a capacitor C_i, and the elements of the local amplifier's equivalent circuit. Each amplifier A_i comprises an input resistance, ρ_i, an output resistance, δ_i, and a controlled generator G_i injecting a current linearly depending on the capacitor C_i's voltage through a gain coefficient k_i. Let $x_i(t)$ be the voltage at time t of the capacitor C_i. Then, the current injected by G_i is $k_i\,x_i(t)$, where $k_i > 0$ if the amplifier works in non-inverting configuration, and $k_i < 0$ if the amplifier is in inverting configuration. The electronic circuit is controlled through an input signal $v(t)$ that is applied at the first RC-branch, while a short circuit is imposed at the last branch. We aim to characterize the propagative properties of a disturbance signal $u(t)$ that is applied at the i-th node.

To this aim, we first determine a dynamical model of the system. By applying Kirchhoff's current law, we obtain the following balance equations:

$$i_{R_i}(t) - i_{C_i}(t) - i_{\rho_i} - i_{G_i}(t) - i_{\delta_i} - i_{R_{i+1}}(t) = 0\,,$$

for $i = 1, 2, \cdots, n$, which can be written in terms of the system's state by exploiting Kirchhoff's voltage law:

$$\frac{1}{R_i}\,(x_{i-1}(t) - x_i(t)) - C_i\,\dot{x}_i(t) - \frac{1}{\rho_i} x_i(t) - k_i\,x_i(t) + \\ - \frac{1}{\delta_i} x_i(t) - \frac{1}{R_{i+1}}\,(x_i(t) - x_{i-1}(t)) = 0\,.$$

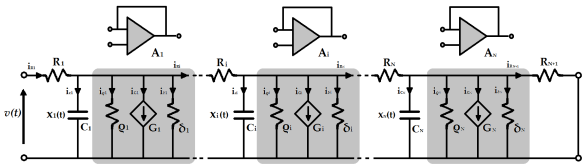

i	R_i [Ω]	C_i [F]	k_i
1	$1 \cdot 10^{0}$	$1.33 \cdot 10^{0}$	$-6.67 \cdot 10^{-2}$
2	$3.75 \cdot 10^{0}$	$3.56 \cdot 10^{-1}$	$-1.78 \cdot 10^{-2}$
3	$1.41 \cdot 10^{1}$	$9.48 \cdot 10^{-2}$	$-4.74 \cdot 10^{-3}$
4	$5.27 \cdot 10^{1}$	$2.53 \cdot 10^{-2}$	$-1.26 \cdot 10^{-3}$
5	$1.98 \cdot 10^{2}$	$6.74 \cdot 10^{-3}$	$-3.36 \cdot 10^{-4}$
6	$7.42 \cdot 10^{2}$	$1.8 \cdot 10^{-3}$	$-8.86 \cdot 10^{-5}$
7	$2.78 \cdot 10^{3}$	$4.79 \cdot 10^{-4}$	$-2.26 \cdot 10^{-5}$
8	$1.04 \cdot 10^{4}$	$1.28 \cdot 10^{-4}$	$-5.06 \cdot 10^{-6}$
9	$3.91 \cdot 10^{4}$	$3.41 \cdot 10^{-5}$	$-3.71 \cdot 10^{-7}$
10	$1.47 \cdot 10^{5}$	$9.09 \cdot 10^{-6}$	$8.79 \cdot 10^{-7}$
	$a = -1$	$b = 0.2$	$c = 0.75$

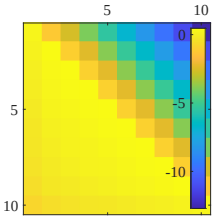

i	R_i [Ω]	C_i [F]	k_i
1	$1 \cdot 10^{10}$	$1 \cdot 10^{-9}$	$1.33 \cdot 10^{-6}$
2	$8.33 \cdot 10^{8}$	$1.2 \cdot 10^{-8}$	$1.34 \cdot 10^{-6}$
3	$6.94 \cdot 10^{7}$	$1.44 \cdot 10^{-7}$	$1.38 \cdot 10^{-6}$
4	$5.79 \cdot 10^{6}$	$1.73 \cdot 10^{-6}$	$1.85 \cdot 10^{-6}$
5	$4.82 \cdot 10^{5}$	$2.07 \cdot 10^{-5}$	$7.55 \cdot 10^{-6}$
6	$4.02 \cdot 10^{4}$	$2.49 \cdot 10^{-4}$	$7.6 \cdot 10^{-5}$
7	$3.35 \cdot 10^{3}$	$2.99 \cdot 10^{-3}$	$8.97 \cdot 10^{-4}$
8	$2.79 \cdot 10^{2}$	$3.58 \cdot 10^{-2}$	$1.08 \cdot 10^{-2}$
9	$2.33 \cdot 10^{1}$	$4.3 \cdot 10^{-1}$	$1.29 \cdot 10^{-1}$
10	$1.94 \cdot 10^{0}$	$5.16 \cdot 10^{0}$	$1.55 \cdot 10^{0}$
	$a = -1$	$b = 1.2$	$c = 0.1$

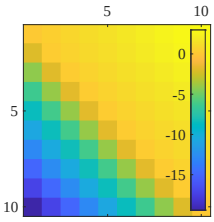

Fig. 4. Electronic network yielding tridiagonal Toeplitz structure: (top row) scheme of the chain of n voltage-feedback transconductance amplifiers; (second and third rows) parameters and heat maps of $\log(|A^{-1}|)$, with $A \in \mathbb{R}^{10\times 10}$, for two networks satisfying conditions 1-b and 2-b, and conditions 1-a and 2-b, of Th. 3.1, respectively. Accordingly, in the former, the sequence of entries is decreasing for $j \geq i$ and increasing for $j < i$, while in the latter, they are increasing for all rows. Note that all network matrices are Hurwitz stable.

The electronic circuit can then be modeled as a network system in Fig. 2 with dynamic equation:

$$\dot{x}_i(t) = c_i\, x_{i-1}(t) + a_i\, x_i(t) \;+\; b_i\, x_{i+1}(t)\,, \qquad (13)$$

where $a_i = -b_i - c_i - \frac{1}{\rho_i\, C_i} - \frac{1}{\delta_i\, C_i} + \frac{k_i}{C_i}$, $b_i = \frac{1}{R_{i+1} C_i} > 0$, and $c_i = \frac{1}{R_i C_i} > 0$. for $i = 1, \cdots, n$, $x_0 = u$ and $x_{n+1} = 0$.

We now study two numerical instances of the above electronic circuit with $n = 10$. For simplicity, we let all input and output resistances of the amplifiers have equal value, that is, $\rho_i = \rho = 1 \cdot 10^6\,\Omega$ and $\delta_i = \delta = 3 \cdot 10^6\,\Omega$. By choosing the other circuit parameters as in the upper table in Fig. 4, the network parameters are such that the network matrix A is Toeplitz and satisfies the conditions 1-b and 2-b in Th. 3.1. Thus, the sequences A^{-1}_{ij}, for $j \geq i$ (respectively $j < i$), show a decreasing (respectively increasing) behavior. Instead, for the circuit parameters reported in the lower table of Fig. 4, the network matrix A satisfies the conditions 1-a and 2-b in Th. 3.1, so that the sequences A^{-1}_{ij} are increasing for all rows i. A graphical illustration of the behaviors of the entries of the inverse of the network matrix is reported in Fig. 4. Accordingly, for the first set of parameters, a disturbance is mostly visible close to the signal source, while for the latter it is greatest at the right extreme of the circuit.

V. Conclusion and Future Work

In this letter we studied the problem of selecting sensor nodes for optimal signal detection in network systems. We adopt the trace of the cross-Gramian or, equivalently for SISO systems, the static gain of the network system, to evaluate different sensor positions with respect to the origin of a signal to be detected. For line networks with Toeplitz or general weights, we show that the entries of the inverse of the network matrix can exhibit drastically different behaviors. Consequently, to maximize the detection performance, the sensor should either be co-located with the origin of the signal, or as far as possible from it, depending on the network parameters. We illustrate our findings through a synthetic example and a class of electronic circuits. Several problems are left as the subject of future research, including the extension to multi-input multi-sensor scenarios, and the study of different network topologies.

References

[1] S. V. Buldyrev, R. Parshani, G. Paul, H. E. Stanley, and S. Havlin, "Catastrophic cascade of failures in interdependent networks," *Nature*, vol. 464, no. 7291, pp. 1025–1028, 2010.

[2] T. Kailath, *Linear Systems*. Prentice-Hall, 1980.

[3] D. Georges, "The use of observability and controllability Gramians or functions for optimal sensor and actuator location in finite-dimensional systems," in *IEEE Conf. on Decision and Control*, New Orleans, LA, USA, Dec. 1995, pp. 3319–3324.

[4] B. Marx, D. Koenig, and D. Georges, "Optimal sensor and actuator location for descriptor systems using generalized Gramians and balanced realizations," in *American Control Conference*, Boston, MA, USA, Jul. 2004, pp. 2729–2734.

[5] R. Anguluri, R. Dhal, S. Roy, and F. Pasqualetti, "Network invariants for optimal input detection," in *American Control Conference*. IEEE, 2016, pp. 3776–3781.

[6] T. H. Summers and J. Lygeros, "Optimal sensor and actuator placement in complex dynamical networks," *IFAC Proceedings Volumes*, vol. 47, no. 3, pp. 3784–3789, 2014.

[7] F. Pasqualetti, S. Zampieri, and F. Bullo, "Controllability metrics, limitations and algorithms for complex networks," *IEEE Transactions on Control of Network Systems*, vol. 1, no. 1, pp. 40–52, 2014.

[8] V. Tzoumas, M. A. Rahimian, G. J. Pappas, and A. Jadbabaie, "Minimal actuator placement with bounds on control effort," *IEEE Trans. on Control of Network Systems*, vol. 3, no. 1, pp. 67–78, 2015.

[9] G. Yan, G. Tsekenis, B. Barzel, J.-J. Slotine, Y.-Y. Liu, and A.-L. Barabási, "Spectrum of controlling and observing complex networks," *Nature Physics*, vol. 11, no. 9, pp. 779–786, 2015.

[10] R. Dhal and S. Roy, "Vulnerability of continuous-time network synchronization processes: A minimum energy perspective," in *IEEE Conf. on Decision and Control*, 2013, pp. 823–828.

[11] Y. Tang, F. Qian, H. Gao, and J. Kurths, "Synchronization in complex networks and its application–a survey of recent advances and challenges," *Ann. Reviews in Control*, vol. 38, no. 2, pp. 184–198, 2014.

[12] C. P. Pfleeger and S. L. Pfleeger, *Security in computing*. Prentice Hall Professional Technical Reference, 2002.

[13] B. Moore, "Principal component analysis in linear systems: Controllability, observability, and model reduction," *IEEE Trans. on Automatic Control*, vol. 26, no. 1, pp. 17–32, Feb 1981.

[14] K. Fernando and H. Nicholson, "On the structure of balanced and other principal representations of siso systems," *IEEE Trans. on Automatic Control*, vol. 28, no. 2, pp. 228–231, Feb 1983.

[15] C. Himpe and M. Ohlberger, "Cross–gramian–based combined state and parameter reduction for large-scale control systems," *Mathematical Problems in Engineering*, 2014.

[16] A. Laub, L. M. Silverman, and M. Verma, "A note on cross–grammians for symmetric realizations," *Proceedings of the IEEE*, vol. 71, no. 7, pp. 904–905, July 1983.

[17] J. W. Lewis, "Inversion of tridiagonal matrices," *Numerische Mathematik*, vol. 38, no. 3, pp. 333–345, 1982.

[18] A. S. Sedra and K. C. Smith, *Microelectronic circuits*. Oxford university press, 1998, vol. 1.